Title
Nicotine plus a high-fat diet triggers cardiomyocyte apoptosis

Journal
Cell and Tissue Research, 368(1)

ISSN
0302-766X

Authors
Sinha-Hikim, Indrani
Friedman, Theodore C
Falz, Mark
et al.

Publication Date
2017-04-01

DOI
10.1007/s00441-016-2536-1

Peer reviewed

HHS Public Access

Author manuscript

Cell Tissue Res. Author manuscript; available in PMC 2018 February 15.

Published in final edited form as:

Cell Tissue Res. 2017 April ; 368(1): 159–170. doi:10.1007/s00441-016-2536-1.

Nicotine plus a high-fat diet triggers cardiomyocyte apoptosis

Indrani Sinha-Hikim[1,2], **Theodore C. Friedman**[1,2], **Mark Falz**[1], **Victor Chalfant**[1], **Mohammad Kamrul Hasan**[1], **Jorge Espinoza-Derout**[1], **Desean L. Lee**[1], **Carl Sims**[1], **Peter Tran**[1], **Sushil K. Mahata**[3], and **Amiya P. Sinha-Hikim**[1,2]

[1]Division of Endocrinology, Metabolism and Molecular Medicine, Department of Internal Medicine, Charles R. Drew University of Medicine and Science, 1731 E. 120th Street, Los Angeles CA 90059, USA

[2]David Geffen School of Medicine at University of California, Los Angeles, Los Angeles CA 90095, USA

[3]VA San Diego Health Care System and University of California, San Diego, Calif., USA

Abstract

Cigarette smoking is an important risk factor for diabetes, cardiovascular disease and non-alcoholic fatty liver disease. The health risk associated with smoking can be aggravated by obesity. Smoking might also trigger cardiomyocyte (CM) apoptosis. Given that CM apoptosis has been implicated as a potential mechanism in the development of cardiomyopathy and heart failure, we characterize the key signaling pathways in nicotine plus high-fat diet (HFD)-induced CM apoptosis. Adult C57BL6 male mice were fed a normal diet (ND) or HFD and received twice-daily intraperitoneal (IP) injections of nicotine (0.75 mg/kg body weight [BW]) or saline for 16 weeks. An additional group of nicotine-treated mice on HFD received twice-daily IP injections of mecamylamine (1 mg/kg BW), a non-selective nicotinic acetylcholine receptor antagonist, for 16 weeks. Nicotine when combined with HFD led to a massive increase in CM apoptosis that was fully prevented by mecamylamine treatment. Induction of CM apoptosis was associated with increased oxidative stress and activation of caspase-2-mediated intrinsic pathway signaling coupled with inactivation of AMP-activated protein kinase (AMPK). Furthermore, nicotine treatment significantly ($P < 0.05$) attenuated the HFD-induced decrease in fibroblast growth factor 21 (FGF21) and silent information regulator 1 (SIRT1). We conclude that nicotine, when combined with HFD, triggers CM apoptosis through the generation of oxidative stress and inactivation of AMPK together with the activation of caspase-2-mediated intrinsic apoptotic signaling independently of FGF21 and SIRT1.

Keywords

Nicotine; High-fat diet; Cardiomyocyte apoptosis; Oxidative stress; Mouse

Introduction

Cigarette smoking is the leading preventable cause of death and disability from various diseases worldwide (He et al. 2005). It is also a major risk factor for cardiovascular disease, chronic obstructive pulmonary disease and lung cancer (Barnes 2003; Zaher et al. 2004;

Hudson and Mannino 2010) and non-alcoholic fatty liver disease (Hamabe et al. 2011; Zein et al. 2011). Importantly, the health risk associated with smoking is aggravated by obesity and smoking and obesity are the leading causes of morbidity and mortality worldwide (Haslam and James 2005; Chiolero et al. 2008).

Many studies have indicated that cardiomyocyte (CM) apoptosis plays a causal role in the morphogenesis and remodeling of the mammalian heart during the first 2 postnatal weeks and have implicated CM apoptosis as a mechanism in the development of cardiac failure of either ischemic or non-ischemic origin (Kajstura et al. 1995; Fernandez et al. 2001; Wencker et al. 2003; Scarabelli and Gottlieb 2004; Foo et al. 2005; Moorjani et al. 2006; Lee and Gustafsson 2009; Mandl et al. 2011). Evidence is growing that nicotine can also trigger CM apoptosis (Yamada et al. 2009; Zhou et al. 2010; Wang et al. 2011). Of note, usages of nicotine-only formulations such as transdermal patches, nicotine gum and electronic cigarettes, in particular, are increasing (Sage Colombo et al. 2013; Grando 2014).

We have previously shown that nicotine when combined with a high-fat diet (HFD) triggers greater oxidative stress, activates hepatocellular apoptosis and amplifies HFD-induced hepatic steatosis (Friedman et al. 2012) and that the caspase-2-mediated intrinsic pathway constitutes a critical component of apoptotic signaling for nicotine and HFD-induced hepatocellular apoptosis (Ivey et al. 2014). Recently, we further demonstrated the detrimental effects of the combined treatment of nicotine and HFD on skeletal muscle (Sinha-Hikim et al. 2014).

In the current study, we test the hypothesis that nicotine in combination with HFD can also induce CM apoptosis through the generation of oxidative stress and the inactivation of AMP-activated protein kinase (AMPK) together with the activation of caspase-2-mediated intrinsic apoptotic signaling. To this end, we fed C57BL/6 J mice with HFD in which 60 % of calories were derived from fat, a commonly used model of diet-induced obesity (Collins et al. 2004; Behan et al. 2010; de Meijer et al. 2010), in the presence or absence of nicotine for 16 weeks.

Materials and methods

Mice and tissue preparation

Male 10-week-old C57BL/6 mice weighing 22–24 g and obtained from Taconic Farms (Germantown, N.Y., USA) were used for all experiments. Mice were housed (2–3 per cage) under controlled temperature (22 °C) and photoperiod (12-h light and 12-h dark cycle) conditions with free access to water and food. Groups of five mice were fed for 16 weeks either a normal diet (ND) with 5 % fat (2.03 kcal/gm; laboratory rodent diet no. 5001; Lab diet, Richmond, Ind., USA) or HFD with 60 % of calories being derived from fat. HFD consisted of 26.2 % protein, 26.3 % carbohydrate and 34.9 % fat (mostly lard, 5.24 kcal/g; D12492; Research Diets, New Brunswick, N.J., USA). Mice on either diet ($n = 5$) received twice-daily intraperitoneal (IP) injections of nicotine (0.75 mg/kg body weight [BW]) or saline for 16 weeks. The rationale for using twice daily IP administration of nicotine (0.75 mg/kg BW) was based on the results of our previous studies, which demonstrated that this dose level of nicotine, when combined with HFD, triggered greater oxidative stress,

activated hepatocellular apoptosis, amplified HFD-induced hepatic steatosis (Friedman et al. 2012) and caused intramyocellular lipid accumulation and intramyofibrillar mitochondrial abnormalities in the skeletal muscle (Sinha-Hikim et al. 2014). Notably, the daily dosage of 1.5 mg/kg BW in mice appeared to be similar to the clinically relevant concentrations found in habitual cigarette smokers and users of nicotine-containing chewing gum (Wu et al. 2015). An additional group of five nicotine-treated mice on HFD received twice-daily IP injections of mecamylamine (1 mg/kg BW), a non-selective nicotinic acetylcholine receptor (nAChR) antagonist, for 16 weeks (Bacher et al. 2009).

Mice were fasted overnight before being killed with a lethal injection of sodium pentobarbital (200 mg/kg BW). At autopsy, ventricles from 5 mice in each experimental group were carefully removed and dissected and portions of the left ventricles were either fixed in 2.5 % glutaraldehyde for high-resolution light and electron microscopy or 4 % formalin for terminal deoxynucleotidyl transferase-mediated deoxyuridine triphosphate nick end labeling (TUNEL) or routine histological, immunohistochemical, or immunofluorescence studies. Five randomly selected left ventricular sections of ~5 μm in thickness and taken 50 μm apart per animal in each group were viewed to obtain the rate of CM apoptosis or for immunohistochemical analysis and computerized densitometry. Moreover, in order to minimize intra-sample variability, ventricular sections from the various experimental groups were processed for either TUNEL or immunolabeling for a given antibody in a single batch by using identical reagents. Altogether, five batches were processed. Portions of glutaraldehyde-fixed left ventricles were further diced into small pieces, post-fixed in 1 % osmium tetroxide and embedded in Epon 812 as described previously (Friedman et al. 2012; Sinha-Hikim et al. 2011a, 2014). Thin sections from selected tissue blocks were cut with an LKB ultramicrotome, stained with uranyl acetate and lead citrate and examined with a Hitachi electron microscope (Hitachi, Indianapolis, Ind., USA). Ventricles from additional groups of 5 mice were quickly removed, snap-frozen in liquid nitrogen and stored at −80 °C for Western blot analysis. Animal handling and experimentation were in accordance with the recommendations of the American Veterinary Medical Association and were approved by the Charles R. Drew University School of Medicine and Science Institutional Animal Care and Use Committee (IACUC).

CM apoptosis

In situ detection of cells with DNA strand breaks was performed in formalin-fixed paraffin-embedded ventricular sections by the TUNEL technique (Sinha-Hikim et al. 2011a) with an ApopTag-peroxidase kit (Chemicon International, San Francisco, Calif., USA). The apoptotic nature of the cell death and the identity of the dying cardiomyocyte were further confirmed by electron microscopy (Friedman et al. 2012; Sinha-Hikim et al. 2011a, 2014). Enumeration of TUNEL-positive (apoptotic) and TUNEL-negative (non-apoptotic) nuclei was carried out in left ventricular sections stained with the ApopTag peroxidase kit by using an American Optical Microscope with a ×40 objective and a pair of ×10 eyepieces. Methyl green was used as a counterstain to detect non-apoptotic nuclei. Quantitation of apoptotic and non-apoptotic nuclei was carried out by using an unbiased two-dimension rule (Cruz-Orive and Weibel 1990) by counting the number of these nuclei within a reference area encompassing 62,500 μm^2 of the left ventricle and provided by fitting one eyepiece with a

square lattice grid (Sinha-Hikim et al. 2011a). For each section, at least 10 grid fields (50 grid fields/mouse) were examined. Only nuclei intersected by inclusion edges (upper and right borders) and within the frame were counted. The rate of CM apoptosis was expressed as the percentage of the TUNEL-positive apoptotic nuclei per total nuclei (apoptotic plus non-apoptotic) present within the reference area (Sinha-Hikim et al. 2011a, 2011b).

Immunohistochemical and immunofluorescence analyses

Formalin-fixed paraffin-embedded left ventricular sections were immunostained as described previously (Sinha-Hikim et al. 2011a, 2011b, 2013; Ivey et al. 2014). Primary antibodies included mouse monoclonal 4-hydroxynonenal protein adducts (4-HNE; 1:100; Oxis International, Foster City, Calif., USA) and rabbit polyclonal phospho-AMP-activated protein kinase (p-AMPK; 1:100; Santa Cruz Biotechnology, Santa Cruz, Calif., USA), fibroblast growth factor 21 (FGF21; 1:50; Abcam, San Francisco, Calif., USA), silent information regulator 1 (SIRT1; 1:50; EMD Millipore Billerica, Mass., USA), active caspase 2 (1:50; Abcam), active caspase 9 (1:50; Novus Biologicals) and active caspase 3 (1:50; Cell ignaling Technology, Beverly, Mass., USA). Immunoreactivity was detected by using biotinylated anti-mouse or anti-rabbit IgG secondary antibody followed by avidin-biotinylated horseradish peroxidase complex and was visualized with diaminobenzidine tetrahydrochloride (DAB) as recommended in the manufacturer's instructions (VECTASTAIN Elite ABC Rabbit IgG kit, Burlingame, Calif., USA). Slides were counterstained with hematoxylin. Negative controls were run for every assay and processed in an identical manner, except the primary antibody was substituted by the mouse or rabbit IgG. Immunoreactivity was quantified by computerized densitometry by using ImagePro Plus, version 5.1 software (Media Cybernetics, Silver Spring, Md., USA) coupled to an Olympus BHS microscope equipped with a VCC video camera as described previously (Sinha-Hikim et al. 2011a). At least 10 test areas were analyzed for each antibody in each of 5 left ventricular sections for a total of 50 test areas per mouse.

Inactivation of AMPK in CMs was detected by fluorescence microscopy by using double-immunostaining with p-AMPK (1:100) and α-actinin (1:100; Santa Cruz Biotechnology), a marker of CM (Kuzmenkin et al. 2009; Jin et al. 2010), as previously described (Friedman et al. 2012; Sinha-Hikim et al. 2011a, 2011b). In brief, after deparaffinization and rehydration, tissue sections were incubated with a rabbit polyclonal phospho-AMPK (1:100) antibody in a humidified chamber overnight at 4 °C followed by donkey-anti-rabbit fluorescein-isothiocyanate-conjugated secondary antibody for 45 min at room temperature. The sections were then incubated with a rabbit polyclonal α-actinin antibody, followed by donkey anti-rabbit Texas Red-labeled secondary antibody for 45 min at room temperature, washed and mounted in ProLong Antifade (Molecular Probes). For controls, sections were treated only with secondary antibody and no signals were detected. Sections were viewed with a Zeiss-Axioscop fluorescence microscope.

Western blotting

Western blotting was performed by using ventricular lysates as described previously (Friedman et al. 2012; Ivey et al. 2014; Sinha-Hikim et al. 2014). In brief, proteins (50–80 μg) were separated on a 4–12 % SDS-polyacrylamide gel with 2-(N-morpholine) ethane

sulfonic acid or 3 (N-morpholino) propane sulfonic acid buffer purchased from Invitrogen (Carlsbad, Calif., USA) at 200 V. Bands were transferred onto an Immuno-blot PVDF Membrane (Bio-Rad, Hercules, Calif., USA) overnight at 4 °C. Membranes were blocked in blocking solution (0.3 % Tween 20 in TRIS-buffered saline [TBS-T] and 10 % non-fat dry milk) for 1 h at room temperature and then probed with rabbit polyclonal phospho-AMPK (1: 300) antibody (Cell Signaling Technology) for 1 h at room temperature or overnight at 4 °C with constant shaking. Following three 10-min washes in TBS-T buffer, membranes were then incubated in anti-rabbit IgG secondary antibody (Amersham Biosciences, Piscataway, N.J., USA) at a 1:2000 dilution. For immunodetection, membranes were washed three times in TBS-T wash buffer, incubated with enhanced chemiluminescence (ECL) solutions as in the manufacturer's specifications (Amersham Biosciences) and exposed to Hyper film ECL. The membranes were stripped and re-probed with a rabbit polyclonal antibody against D-glyceraldehyde-3-phosphate dehydrogenase (1:2000) from Millipore (Billerica, Mass., USA) for normalization of the loading. Band intensities were determined using Quantity One software from Bio-Rad.

Statistical analysis

Statistical analyses were performed by using the SigmaStat 2.0 Program (Jandel Corporation, San Rafael, Calif., USA). Data are presented as means ± SEM. We used one-way analysis of variance (ANOVA) to assess the statistically significant differences among various treatment groups. If overall ANOVA revealed significant differences, post-hoc (pairwise) comparisons were performed by using Tukey's tests. Differences were considered significant if $P < 0.05$.

Results

Nicotine plus HFD triggers CM apoptosis

We first examined the additive effects of nicotine and HFD on CM apoptosis (Fig. 1a–h). Compared with mice fed on ND in the absence (Fig. 1a) or presence (Fig. 1b) of nicotine or on HFD (Fig. 1c) alone, when little or no apoptosis was detected, combined treatment with nicotine and HFD resulted in a marked increase in the incidence of apoptosis (Fig. 1d). Treatment with mecamylamine, a non-selective nAChR antagonist significantly ($P < 0.05$) prevented nicotine-plus-HFD-induced CM apoptosis (Fig. 1e). Electron microscopic observation further confirmed the apoptotic nature and the identity of dying cells as cardiomyocytes (Fig. 1f, g). As shown in Fig. 1h, a low incidence, expressed as the percentage of TUNEL-positive nuclei per total (apoptotic plus non-apoptotic) nuclei, of CM apoptosis was noted in mice on ND in the absence (0.4 ± 0.2) or presence (3.5 ± 1.7) of nicotine or in mice fed on HFD alone (3.8 ± 0.3). However, combined with HFD, nicotine led to a significant ($P < 0.05$) increase in CM apoptosis (18.7 ± 6.9). Notably, mecamylamine treatment suppressed CM apoptosis to levels comparable with that seen in mice fed on ND with or without nicotine or fed on HFD alone.

Nicotine plus HFD inactivates AMPK and triggers oxidative stress

AMPK, a major cellular energy sensor and a master regulator of metabolic homeostasis, plays an important role in regulating CM apoptosis and is an essential component of the

adaptive response to CM stress (Zhang et al. 2009; Zhuo et al. 2013; Guo et al. 2015; Qi and Young 2015). To investigate whether nicotine-plus-HFD-induced CM apoptosis is associated with the inactivation of AMPK, we compared the in vivo expression of ventricular phospho-AMPK in various treatment groups (Fig. 2a–h). Compared with mice fed on ND without (Fig. 2a) or with (Fig. 2b) nicotine or on HFD (Fig. 2c) alone, combined treatment with nicotine and HFD resulted in a significant ($P < 0.05$) decrease (by 39.0 % relative to the values measured in mice on ND) in phospho-AMPK immunoreactivity, as shown by image analysis of staining intensity (Fig. 2d, f). Treatment with mecamylamine significantly ($P < 0.05$) attenuated the nicotine-plus-HFD-induced decrease in phospho-AMPK levels (Fig. 2e, f). Western blot analysis also revealed a marked decrease in phospho-AMPK levels following nicotine plus HFD treatment compared with mice fed on ND with or without nicotine or on HFD alone (Fig. 2g). Densitometric analysis further revealed a significant ($P < 0.05$) decrease (by 50.6 %) of phospho-AMPK in the combined treatment group as compared with mice fed HFD alone. Co-staining for α-actinin, a cardiac myocyte marker (Kuzmenkin et al. 2009; Jin et al. 2010) further confirmed the localization of phospho-AMPK in cardiomyocytes (Fig. 2hI–VI) and showed a decreased expression of phospho-AMPK levels after combined treatment with nicotine plus HFD in cardiomyocytes (Fig. 2hIV–VI).

To test whether nicotine plus HFD caused greater oxidative stress, we compared the in vivo expression of a lipid peroxidation product, namely 4-HNE (Fig. 3a–f), a biomarker of oxidative stress (Kohen and Nysks 2002; Tam et al. 2003). Compared with mice fed on ND (Fig. 3a), when no 4-HNE immunoreactivity was detected, nicotine treatment led to a modest (2.2-fold) but significant ($P < 0.05$) increase in the expression of 4-HNE (Fig. 3b, f). As shown in Fig. 3c, f, ventricular 4HNE expression also increased significantly ($P < 0.05$) by 3.4-fold (over the values measured in mice on ND) in mice fed on HFD. When combined, nicotine plus HFD caused a further increase (1.5-fold over the values measured in HFD-fed mice) in ventricular 4-HNE expression (Fig. 3d, f). Treatment with mecamylamine fully prevented the nicotine-plus-HFD-induced increase in 4-HNE immunoreactivity, similar to the levels seen in nicotine-treated mice on ND (Fig. 3e, f).

Nicotine-plus-HFD-induced CM apoptosis is associated with activation of caspases

Because caspase 2 works upstream of kinase activation and the mitochondria-dependent apoptotic pathway (Lassus et al. 2002; Johnson et al. 2008), we visualized caspase 2 activation by immunohistochemistry (Fig. 4a–a‴). Image analysis of active caspase 2 staining intensity revealed that nicotine significantly ($P < 0.05$) increased ventricular active caspase 2 expression in mice fed either on ND (by 9.8-fold) or on HFD (9.5-fold) relative to mice fed on ND (Fig. 4a–a‴, d). We next examined the role of downstream caspases in nicotine-plus-HFD-induced CM apoptosis. Compared with mice on ND, when no active caspase 9 (Fig. 4b, b′, d) or caspase 3 immunoreactivity (Fig. 4c, c′, d″) was detected, we found a marked increase in the ventricular expression of both active caspases 9 (by 6.6-fold; Fig. 4b″, d′) and caspase 3 (by 4.3-fold; Fig. 4c″, d″) in mice fed with HFD. A further significant ($P < 0.05$) increase (over the values measured in HFD-fed mice) in ventricular expression of active caspase 9 (1.4-fold) and caspase 3 (2.3-fold) was noted in the combined treatment group (Fig. 4b‴, d′, c‴, d″, respectively).

Nicotine treatment attenuates HFD-induced inhibition of FGF21 and SIRT1

Given that FGF21 plays an important role in cardiac protection against various insults and cardiovascular disease (Planavila et al. 2015; Tanajak et al. 2015; Zhang et al. 2015), we next examined the effect of nicotine plus HFD on the ventricular expression of FGF21 (Fig. 5a–a‴′, c). No difference was seen in FGF21 immunoreactivity in mice fed on ND in the absence (Fig. 5a, c) or presence (Fig. 5a′, c) of nicotine. Compared with mice fed on ND, mice on HFD exhibited a marked decrease in the ventricular expression of FGF21 by 60.0 % (Fig. 5a″, c). Combined treatment with nicotine and HFD fully prevented such an HFD-induced decrease in the ventricular expression of FGF21 (Fig. 5a‴, c). Treatment with mecamylamine led to a decrease in FGF21 immunoreactivity by 50.0 %, which was comparable with levels seen in ventricles from HFD-fed mice (Fig. 5a‴′, c), indicating that nicotine has a direct role in reversing HFD-induced reduction in ventricular FGF21 immunoreactivity.

SIRT1, a nicotinamide-adenine-dinucleotide-dependent histone deacetylase, plays a major role in counteracting CM apoptosis and provides protection against various diseases, including cardiovascular disease (Herranz and Serrano 2010; Cattelan et al. 2015; Ding et al. 2015). Accordingly, we next examined the effect nicotine plus HFD had on the ventricular expression of SIRT1 (Fig. 5b–b‴′, d). No difference was observed in SIRT1 immunoreactivity in mice fed on ND in the absence (Fig. 5b, d) or presence (Fig. 5b′, d) of nicotine. Compared with mice fed on ND, mice on HFD exhibited a marked decrease (by 22 %) in the ventricular expression of SIRT1 (Fig. 5b″, d). Combined treatment with nicotine and HFD, however, fully prevented such an HFD-induced decrease in the ventricular expression of SIRT1 (Fig. 5b‴, d). As shown in Fig. 5b‴′, d, treatment with mecamylamine led to a decrease in SIRT1 immunoreactivity by 21 %; this was identical to that seen in ventricles from HFD-fed mice (Fig. 5b″, d) indicating that nicotine had a direct role in Treatment with mecamylamine restored the decrease in FGF21 (**a**‴′) and SIRT1 (**b**‴′) immunoreactivity to levels comparable with that seen in ventricles from HFD-fed mice (**a**″, **b**″). *Bar* 25 μm. **c**, **d** Quantitation of staining intensities for FGF21 (**c**) and SIRT1 (**d**). Values are means ± SEM of 5 mice and were taken from 10 test areas in each of 5 ventricular sections for a total of 50 test areas per mouse. Means with unlike superscripts are significantly ($P < 0.05$) different reversing HFD-induced reduction in ventricular SIRT1 immunoreactivity.

Discussion

CM apoptosis has been implicated as a mechanism in the development of cardiac failure of either ischemic or non-ischemic origin (Kajstura et al. 1995; Fernandez et al. 2001; Wencker et al. 2003; Scarabelli and Gottlieb 2004; Foo et al. 2005; Moorjani et al. 2006; Lee and Gustafsson 2009; Mandl et al. 2011). Indeed, Wencker and colleagues (2003), using transgenic mice with inducible CM apoptosis, demonstrated that low levels of apoptosis (levels that are 4.0-fold to 10-fold lower than those seen in human heart failure cases) are sufficient to cause lethal dilated cardiomyopathy. Conversely, the inhibition of CM apoptosis in this murine model largely prevents the development of this syndrome (Wencker et al. 2003). Despite the recognition that the inhibition of CM apoptosis is a logical target for

novel therapies for preventing heart failure (Foo et al. 2005; Lee and Gustafsson 2009), little is known about the mechanisms by which nicotine plus HFD triggers CM apoptosis. An understanding of these mechanisms is indispensable for the rational design of anti-apoptotic therapies.

In this study, we used a model of diet-induced obesity in C57BL6J mice to examine the underlying mechanisms of the detrimental effects of two common lifestyle factors, namely nicotine and HFD, on CM apoptosis. Our data constitute the first demonstration that (1) nicotine plus HFD triggers CM apoptosis, adding cardiac abnormalities to the list of liver and muscle abnormalities that nicotine plus HFD is known to cause (Friedman et al. 2012; Ivey et al. 2014; Sinha-Hikim et al. 2014) and (2) the detrimental effects of nicotine and HFD on CM apoptosis are associated with increased oxidative stress and the activation of intrinsic pathway signaling coupled with the inactivation of AMPK independently of FGF21 and SIRT1.

Oxidative stress has been implicated in apoptotic signaling in various cell types, including cardiomyocytes (Zhou et al. 2010; Sinha-Hikim et al. 2011a; Guo et al. 2015; Sun et al. 2006). Consistent with the role of oxidative stress in CM apoptosis, we found, in the present study, that the combined treatment of nicotine plus HFD generates greater oxidative stress, as evidenced by increase ventricular 4-HNE expression compared with either treatment alone. This is consistent with our previous data showing that both nicotine and HFD are capable of generating oxidative stress in the liver but only when combined, nicotine plus HFD can cause greater oxidative stress (Friedman et al. 2012). Noatbly, in the heart as in the liver (Friedman et al. 2012; Ivey et al. 2014) and in spite of a significant increase in oxidative stress, no change occurs in the incidence of CM apoptosis in mice fed on HFD alone suggesting that the oxidative stress generated by HFD alone is not severe enough to trigger CM apoptosis. This is consistent with earlier reports indicating that cellular responses to oxidative stress vary depending on the cell type, the levels of stress achieved and the duration of exposure (Videla 2010). However, we cannot rule out the possibility that, in addition to high levels of oxidative stress, other factors also contribute to increased CM apoptosis triggered by the combined treatment with nicotine and HFD.

One possible mechanism by which oxidative stress can induce CM apoptosis in response to HFD plus nicotine is through the stimulation of caspase-2-mediated intrinsic pathway signaling (Lassus et al. 2002; Braga et al. 2008; Prasad et al. 2006; Tamm et al. 2008). Interestingly, nicotine significantly ($P < 0.05$) increases active caspase 2 immunostaining in mice fed either on ND or on HFD. This observation rsises the question as to why CMs from ND-fed mice do not undergo apoptosis, in spite of the enhanced expression of caspase 2. One possibility is that caspase 2 is dispensable for nicotine-plus-HFD-induced CM apoptosis. A growing body of evidence indicates that an apoptosis repressor with caspase recruitment domain (ARC) is an endogenous apoptosis repressor protein that is highly expressed in cardiac tissue and that has the ability to inhibit ischemia-reperfusion (I-R)-induced CM apoptosis by targeting the activation of the intrinsic pathway at multiple points (Zhang and Herman 2006; Ludwig-Galezowski et al. 2011; Le et al. 2012). Conversely, the preservation of ARC levels is sufficient for CM viability after oxidative stress (Nam et al. 2007) or infarction (Foo et al. 2007). Available evidence further suggests that, in addition to

ARC, other anti-apoptotic proteins such as BCL-2 and XIAP must be decreased for CM apoptosis to proceed, at least during myocardial I-R injury (Le et al. 2012). ARC activation also counteracts the pro-apoptotic protein BAX (Gustafsson et al. 2002). Thus, one can assume that the induction of CM apoptosis in response to treatment with nicotine plus HFD is only possible in mice if the activation of caspase 2 is also accompanied by a reduced expression of anti-apoptotic proteins, such as XIAP and ARC, coupled with the perturbation of the BAX/BCL-2 ratio. Relevant to this is the demonstration that the perturbation of the BAX/BCL-2 ratio in hepatocytes is only found during nicotine-plus-HFD-induced hepatocellular apoptosis as opposed to individual treatment (Ivey et al. 2014). Furthermore, caspase 2 activation only in the combined treatment group is associated with the activation of downstream caspase 9 (the key initiator caspase in the intrinsic pathway signaling) and caspase 3. It also indicates the involvement of the mitochondria-dependent death pathway in nicotine-plus-HFD-induced CM apoptosis. This is consistent with the previous report showing the involvement of the mitochondria-dependent pathway in I-R-induced CM apoptosis (Le et al. 2012). The data reported herein also indicate that the nicotine-plus-HFD-induced CM apoptosis coincides with the increased expression of FGF21 and SIRT1. Conversely, in spite of a significant ($P < 0.05$) decrease in FGF21 and SIRT1 levels in HFD-fed mice, we found no significant ($P < 0.05$) increase in the incidence of CM apoptosis compared with that in mice on ND in the absence or presence of nicotine. Collectively, these results suggest that the SIRT1 and FGF21 pathway is not involved in nicotine-plus-HFD-induced CM apoptosis.

AMPK, a major cellular energy sensor and a master regulator of metabolic homeostasis, plays an important role in regulating CM apoptosis and is an essential component of the adaptive response to CM stress (Zhang et al. 2009; Zhuo et al. 2013; Guo et al. 2015; Qi and Young 2015). Consistent with the pivotal role of AMPK in myocardial cell apoptosis, we show here that nicotine plus HFD causes significant inhibition (dephosphorylation) of AMPK. This is consistent with our earlier reports that nicotine when combined with a HFD causes the inhibition of AMPK in the liver (Friedman et al. 2012) and in skeletal muscle (Sinha-Hikim et al. 2014). In this context, we should note that isoproterenol instigates CM apoptosis and heart failure via the inactivation of AMPK but can be blocked by AMPK activation (Zhuo et al. 2013), whereas the activation of AMPK by berberine can reduce I-R-induced CM apoptosis in diabetic rats (Chen et al. 2014). Of further interest, emerging evidence suggests that the inhibition of AMPK can also elevate oxidative stress in a variety of cell systems, including cardiac myocytes (Jia et al. 2011; Park et al. 2012; Jeon et al. 2012). Thus, the inhibition of AMPK, through the generation of oxidative stress, might promote nicotine-plus-HFD-induced CM apoptosis.

In summary, we have provided insights into the molecular mechanisms by which nicotine plus HFD triggers CM apoptosis (Fig. 6). We conclude that (1) nicotine plus HFD triggers CM apoptosis and (2) the detrimental effects of nicotine and HFD on the heart are associated with increased oxidative stress and the activation of intrinsic pathway signaling coupled with the inactivation of AMPK independently of FGF21 and SIRT1. Furthermore, our data suggest a direct role of nicotine on cardiac SIRT1-FGF21-AMPK signaling in mice fed HFD. Indeed, nicotinic receptors are present in the heart (Ni et al. 2010; Jutkiewicz et al.

2013). The clinical implication of this study is that smoking plus HFD lead to heart failure and other forms of cardiomyopathy and that anti-apoptotic agents might help to prevent this.

Acknowledgments

This work was supported by the Diversity Promoting Institution Drug Abuse Research Program (DIDARP) grant (R24DA017298) and the Accelerating Excellence in Translational Science (AXIS) grant (2U54MD007598) from the National Institutes of Health (NIH). We also thank the Technology Core of the AXIS grant (2U54MD007598) from NIH for tissue preparation and for hematoxylin and eosin staining.

References

Bacher I, Wu B, Shytle DR, George TP. Mecamylamine—a nicotinic acetylcholine receptor antagonist with potential for the treatment of neuropsychiatric disorders. Expert Opin Pharmacother. 2009; 10:2709–2721. [PubMed: 19874251]

Barnes PJ. New concepts in chronic obstructive pulmonary disease. Annu Rev Med. 2003; 54:113–129. [PubMed: 12359824]

Behan JW, Avramis VI, Yun JP, Louie SG, Mittelman SD. Diet-induced obesity alters vincristine pharmacokinetics in blood and tissues of mice. Pharmacol Res. 2010; 61:385–390. [PubMed: 20083201]

Braga M, Sinha Hikim AP, Datta S, Ferrini M, Brown D, Kovacheva EL, Gonzalez-Cadavid NF, Sinha-Hikim I. Involvement of oxidative stress and caspase 2-mediated intrinsic pathway signaling in age-related increase in muscle cell apoptosis in mice. Apoptosis. 2008; 13:822–832. [PubMed: 18461459]

Cattelan A, Ceolotto G, Bova S, Albiero M, Kuppusamy M, Martin AD, Semplicini A, Fadini GP, de Kreutzenberg SV, Avogaro A. NAD^+-dependent SIRT1 deactvation has a key role on ischemia-reperfusion-induced apoptosis. Vasc Pharmacol. 2015; 70:35–44.

Chen K, Li G, Geng F, Zhang Z, Li J, Yang M, Dong L, Gao F. Berberine reduces ischemia/reperfusion-induced myocardial apoptosis via activating AMPK and PI3K-Akt signaling in diabetic rats. Apoptosis. 2014; 19:946–957. [PubMed: 24664781]

Chiolero A, Faeh D, Paccaud F, Cornuz J. Consequences of smoking for body weight, body fat distribution, and insulin resistance. Am J Clin Nutr. 2008; 87:801–809. [PubMed: 18400700]

Collins S, Martin TL, Surwit RS, Robidoux J. Genetic vulnerability to diet-induced obesity in the C57BL/6J mouse: physiological and molecular characteristics. Physiol Behav. 2004; 81:243–248. [PubMed: 15159170]

Colombo S, Davis J, Makvandi M, Aragon M, Lucas SN, Paffett ML, Campen MJ. Effects of nicotine on cardiovascular remodeling in a mouse model of systemic hypertension. Cardiovasc Toxicol. 2013; 13:364–369. [PubMed: 23959951]

Cruz-Orive LM, Weibel ER. Recent stereological methods for cell biology: a brief survey. Am J Physiol. 1990; 258:L148–L156. [PubMed: 2185653]

Ding M, Lei J, Han H, Li W, Qu Y, Fu E, Fu F. SIRT1 protects against myocardial ischemia-reperfusion injury via activation eNOS in diabetic rats. Cardiovasc Diabetol. 2015; 14:143. [PubMed: 26489513]

Fernandez E, Siddiquee Z, Shohet RV. Apoptosis and proliferation in the neonatal murine heart. Dev Dyn. 2001; 221:302–310. [PubMed: 11458390]

Foo RS-Y, Mani K, Kitsis RN. Death begins failure in the heart. J Clin Invest. 2005; 115:565–571. [PubMed: 15765138]

Foo RS-Y, Chan LKW, Kitsis RN, Bennett MR. Ubiquitination and degradation of the anti-apoptotic protein ARC by MDM2. J Bio Chem. 2007; 282:5529–5535. [PubMed: 17142834]

Friedman TC, Sinha-Hikim I, Parveen M, Najjar SM, Liu Y, Mangubat M, Shin C-S, Lyzlov A, Ivey R, Shaheen M, French SW, Sinha-Hikim AP. Additive effects of nicotine and high-fat diet on hepatic steatosis in male mice. Endocrinology. 2012; 153:5809–5820. [PubMed: 23093702]

Grando SA. Connections of nicotine to cancer. Nat Rev. 2014; 14:419–429.

Guo S, Yao Q, Ke Z, Chen H, Wu J, Liu C. Resveratrol attenuates high glucose-induced oxidative stress and cardiomyocyte apoptosis through AMPK. Mol Cell Endocrinol. 2015; 412:85–94. [PubMed: 26054749]

Gustafsson AB, Sayen MR, Williams SD, Crow MT, Gottlieb RA. TAT protein transduction into isolated perfused hearts: TAT-apoptosis repressor with caspase recruitment domain is cardioprotective. Circulation. 2002; 106:735–739. [PubMed: 12163436]

Hamabe A, Uto H, Imamura Y, Kusano K, Mawatari S, Kumagai K, Kure T, Tamai T, Moriuchi A, Sakiyama T, Oketani M, Ido A, Tsubouchi H. Impact of cigarette smoking on onset of nonalcoholic fatty liver disease over a 10-year period. J Gastroenterol. 2011; 46:769–778. [PubMed: 21302121]

Haslam DW, James WP. Obesity. Lancet. 2005; 366:1197–1209. [PubMed: 16198769]

He J, Gu D, Wu XRK, Duan X, Yao C, Wang J, Chen CS, Chen J, Wildman RP, Klag MJ, Whelton PK. Major causes of death among men and women in China. N Engl J Med. 2005; 353:1124–1134. [PubMed: 16162883]

Herranz D, Serrano M. SIRT1: recent lessons from mouse models. Nat Rev. 2010; 10:819–823.

Hudson NL, Mannino DM. Tobacco use: a chronic illness? J Community Health. 2010; 35:549–553. [PubMed: 20177752]

Ivey R, Desai M, Green K, Sinha-Hikim I, Friedman TC, Sinha-Hikim AP. Additive effects of nicotine and high-fat diet on hepatocellular apoptosis in mice: involvement of caspase 2 and inducible nitric oxide synthase-mediated intrinsic pathway signaling. Horm Metab Res. 2014; 46:568–573. [PubMed: 24830635]

Jeon SM, Chandel NS, Hay N. AMPK regulates NADPH homeostasis to promote tumor cell survival during energy stress. Nature. 2012; 485:661–665. [PubMed: 22660331]

Jia F, Wu C, Chen Z, Lu G. AMP-activated protein kinase inhibits homocysteine-induced dysfunction and apoptosis in endothelial progenitor cells. Cardiovasc Drugs Ther. 2011; 25:21–29. [PubMed: 21258964]

Jin M-S, Shi S, Zhang Y, Yan Y, Sun X-D, Liu W, Liu H-W. Icariin-mediated differentiation of mouse adipose-derived stem cells into cardiomyocytes. Mol Cell Biochem. 2010; 344:1–9. [PubMed: 20563742]

Johnson C, Jia Y, Wang C, Lue YH, Swerdloff RS, Zhang X-S, Hu Z-Y, Li Y-X, Liu Y-X, Sinha-Hikim AP. Role of caspase 2 in apoptotic signaling in primate and murine germ cells. Biol Reprod. 2008; 79:806–814. [PubMed: 18614702]

Jutkiewicz EM, Rice KC, Carroll FI, Woods JH. Patterns of nicotinic receptor antagonism. II. Cardiovascular effects in rats. Drug Alcohol Depend. 2013; 131:284–297. [PubMed: 23333294]

Kajstura J, Mansukhani M, Cheng W, Reiss K, Krajewski S, Reed JC, Qiaini F, Sonnenblick EH, Anversa P. Programmed cell death and expression of the protooncogene bcl-2 in myocytes during post-natal maturation of the heart. Exp Cell Res. 1995; 219:110–121. [PubMed: 7628527]

Kohen R, Nysks A. Oxidation of biological systems: oxidative stress phenomena, antioxidants, redox reaction, and methods for their quantification. Toxicol Pathol. 2002; 30:620–650. [PubMed: 12512863]

Kuzmenkin A, Liang H, Xu G, Pfannkuche K, Eichhorn H, Fatima A, Luo H, Saric T, Werning M, Jaenisch R, Hescheler J. Functional characterization of cardiomyocytes derived from murine induced pluripotent cells in vitro. FASEB J. 2009; 23:4168–4180. [PubMed: 19703934]

Lassus P, Opitz-Araya X, Lazebnik Y. Requirement for caspase-2 in stress-induced apoptosis before mitochondrial permeabilization. Science. 2002; 297:1352–1354. [PubMed: 12193789]

Le TH, Mardini M, Howell VM, Funder JW, Ashton AW, Mihailidou AS. Low-dose spironolactone prevents apoptosis repressor with caspase recruitment domain degradation during myocardial infarction. Hypertension. 2012; 59:1164–1169. [PubMed: 22508833]

Lee Y, Gustafsson AB. Role of apoptosis in cardiovascular disease. Apoptosis. 2009; 14:536–548. [PubMed: 19142731]

Ludwig-Galezowski A, Flanagan L, Rehm M. Apoptosis repressor with caspase recruitment domain, a multifunctional modulator of cell death. J Cell Mol Med. 2011; 15:1044–1053. [PubMed: 21129150]

Mandl A, Pham L, Toth K, Zambetti G, Erhardt P. Puma deletion delays cardiac dysfunction in murine heart failure models through attenuation of apoptosis. Circulation. 2011; 124:31–39. [PubMed: 21670227]

de Meijer VE, Le HD, Meisel JA, Akhavan Sharif MR, Pan A, Nose V, Puder M. Dietary fat intake promotes the development of hepatic steatosis independently from excess caloric consumption in a murine model. Metab Clin Exp. 2010; 59:1092–1105. [PubMed: 20060143]

Moorjani N, Ahmad M, Catarino P, Brittin R, Trabzuni D, Al-Mohanna F, Narula N, Natula J, Westaby S. Activation of apoptotic caspase cascade during the transition to pressure overload-induced heart failure. J Am Coll Cardiol. 2006; 48:1451–1458. [PubMed: 17010810]

Nam Y-J, Mani K, Wu L, Peng C-F, Calvert JW, Foo RS-Y, Krishnamurthy B, Miao W, Ashton AW, Lefer DJ, Kitsis RN. The apoptosis inhibitor ARC undergoes ubiquitin-proteasomal-mediated degradation in response to death stimuli: identification of a degradation resistant mutant. J Biol Chem. 2007; 282:5522–5528. [PubMed: 17142452]

Ni M, Yang Z-W, Li D-J, Li Q, Zhang S-H, Su D-F, Xie H-H, Shen F-M. A potential role of alpha-7 nicotinic acetylcholine receptor in cardiac angiogenesis in a pressor-overload rat model. J Pharmacol Sci. 2010; 114:311–319. [PubMed: 21099147]

Park CS, Bang BR, Kwon HS, Moon KA, Kim TB, Lee KY, Moon HB, Cho YS. Metformin reduces airway inflammation and remodeling via activation of AMP-activated protein kinase. Biochem Pharmacol. 2012; 84:1660–1670. [PubMed: 23041647]

Planavila A, Redondo-Angulo I, Ribas F, Garrabou G, Casademont J, Giralt M, Villarroya F. Fibroblast growth factor 21 protects heart from oxidative stress. Cardiovasc Res. 2015; 106:19–31. [PubMed: 25538153]

Prasad V, Chandele A, Jagtap JC, Kumar S, Shastry P. ROS-triggered caspase 2 activation and feedback amplification loop in b-carotene-induced apoptosis. Free Radic Biol Med. 2006; 41:431–442. [PubMed: 16843824]

Qi D, Young LH. AMPK: energy sensor and survival mechanism in the ischemic heart. Trends Endocrinol Metab. 2015; 26:422–429. [PubMed: 26160707]

Scarabelli TM, Gottlieb RA. Functional and clinical repercussions pf myocyte apoptosis in the multifaceted damage by ischemia/reperfusion injury: old and new concepts after 10 years of contributions. Cell Death Differ. 2004; 11:S144–S152. [PubMed: 15608693]

Sinha-Hikim I, Shen R, Nzenwa I, Gelfand R, Mahata SK, Sinha-Hikim AP. Minocycline suppresses oxidative stress and attenuates fetal cardiac myocyte apoptosis triggered by in utero cocaine exposure. Apoptosis. 2011a; 16:563–573. [PubMed: 21424555]

Sinha-Hikim I, Sinha-Hikim AP, Shen R, Kim H, French SW, Vaziri ND, Crum A, Rajavashisth TB, Norris KC. A novel cystine based antioxidant attenuates oxidative stress and hepatic steatosis in diet-induced obese mice. Exp Mol Pathol. 2011b; 91:419–428. [PubMed: 21570964]

Sinha-Hikim I, Sinha-Hikim AP, Parveen M, Shen R, Goswami R, Tran P, Crum AC, Norris KC. Long-term supplementation with a cystine-based antioxidant delays loss of muscle mass in aging. J Gerontrol A Biol Sci Med Sci. 2013; 68:749–759.

Sinha-Hikim I, Friedman TC, Shin C-S, Lee D, Ivey R, Sinha-Hikim AP. Nicotine in combination with a high-fat diet causes intramyocellular mitochondrial abnormalities in male mice. Endocrinology. 2014; 155:865–872. [PubMed: 24424058]

Sun H-Y, Wang N-P, Halkos M, Kerendi F, Kin H, Guyton RA, Vinten-Johansen J, Zhao Z-Q. Postconditioning attenuates cardiomyocyte apoptosis via inhibition of JNK and p38 mitogen-activated protein kinase signaling. Apoptosis. 2006; 11:1583–1593. [PubMed: 16820962]

Tam NNC, Gao Y, Leung Y-K, Ho S-M. Androgenic regulation of oxidative stress in the rat prostate: involvement of NAD(P)H oxidases and antioxidant defense machinery during prostatic involution and regrowth. Am J Pathol. 2003; 163:2513–2522. [PubMed: 14633623]

Tamm C, Zhivotovsky B, Ceccatelli S. Caspase-2 activation in neural stem cells undergoing stress-induced apoptosis. Apoptosis. 2008; 13:354–363. [PubMed: 18181021]

Tanajak P, Chattipakorn SC, Chittipakorn N. Effects of fibroblast growth factor 21 on the heart. J Endocrinol. 2015; 227:R13–R30. [PubMed: 26341481]

Videla LA. Cytoprotective and suicidal signaling in oxidative stress. Biol Res. 2010; 43:363–369. [PubMed: 21249309]

Wang L, Li X, Zhou Y, Shi H, Xu C, He H, Wang S, Xiong X, Zhang Y, Du Z, Zhang R, Lu Y, Yang B, Shan H. Downregulation of miR-133 via MAPK/ERK signaling pathway involved in nicotine-induce cardiomyocyte apoptosis. Naunyn-Schimiedeberg's Arch Pharamacol. 2011; 387:197–206.

Wencker D, Chandra M, Nguyen K, Miao W, Garantziotis S, Factor SM, Shirani J, Armstrong RC, Kitsis RN. A mechanistic role of cardiac myocyte apoptosis in heart failure. J Clin Invest. 2003; 111:497–1504. [PubMed: 12588888]

Wu Y, Song P, Zhang W, Liu J, Dai X, Liu Z, Lu Q, Ouyang C, Xie Z, Zhao Z, Zhuo X, Viollet B, Foretz M, Wu JYuan Z, Zou M-H. Activation of AMPK a2 in adipocytes is essential for nicotine-induced insulin resistance in vivo. Nat Med. 2015; 21:373–382. [PubMed: 25799226]

Yamada S, Zhang XQ, Kadono T, Matsuoka N, Rollins D, Badger T, Rodesch CK, Barry WT. Direct toxic effects of aqueous extract of cigarette smoke on cardiac myocytes at clinically relevant concentrations. Toxicol Appl Pharmacol. 2009; 236:71–77. [PubMed: 19371621]

Zaher C, Halbert R, Dubios R, George D, Nonikov D. Smoking-related diseases: the importance of COPD. Int J Tuberc Lung Dis. 2004; 8:1423–1428. [PubMed: 15636487]

Zein CO, Unalp A, Colvin R, Liu Y-C, McCullough AJ. Smoking and severity of hepatic fibrosis in nonalcoholic fatty liver disease. J Hepatol. 2011; 54:753–759. [PubMed: 21126792]

Zhang BB, Zhou G, Li C. AMPK: an emerging drug target for diabetes and the metabolic syndrome. Cell Metab. 2009; 9:407–416. [PubMed: 19416711]

Zhang C, Huang Z, Gu J, Yan X, Lu X, Zhou S, Wang S, Shao M, Zhang F, Cheng P, Feng W, Tan Y, Li X. Fibroblast growth factor 21 protects heart from apoptosis in diabetic mouse model via extracellular signal-regulated kinase 1/2-dependent signaling pathway. Diabetologia. 2015; 58:1937–1948. [PubMed: 26040473]

Zhang YQ, Herman B. ARC protects rat cardio myocytes against oxidative stress through inhibition of caspase 2-mediated mitochon-drial pathway. J Cell Biochem. 2006; 99:575–588. [PubMed: 16639714]

Zhou X, Sheng Y, Yang R, Kong X. Nicotine promotes cardiomyocyte apoptosis via oxidative stress and altered apoptosis-related gene expression. Cardiology. 2010; 115:243–250. [PubMed: 20339300]

Zhuo X-Z, Wu Y, Ni J-H, Liu J, Gong M, Wang X-H, Wei F, Wang T-Z, Yuan Z, Ma A-Q, Song P. Isoproterenol instigates cardiomyocyte apoptosis and heart failure via AMPK inactivation–mediated endoplasmic reticulum stress. Apoptosis. 2013; 18:800–810. [PubMed: 23620435]

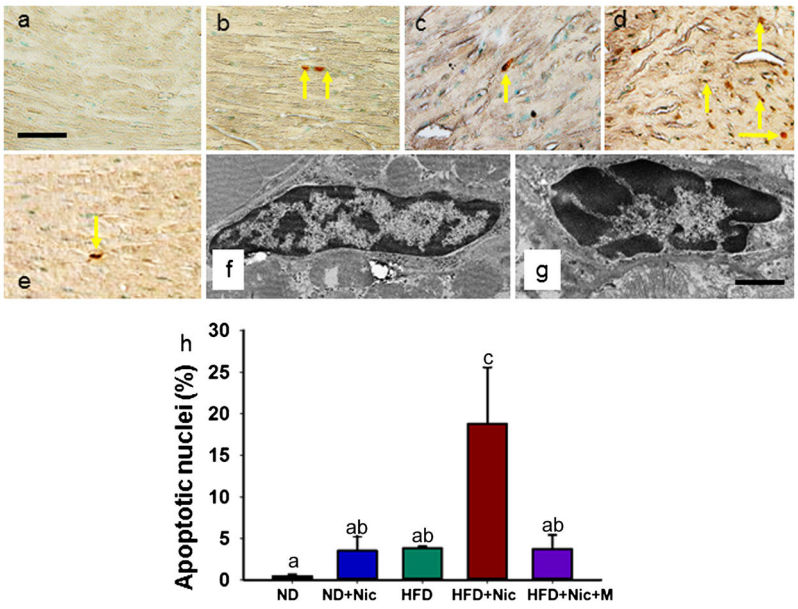

Fig. 1.

In situ detection of cardiomyocyte (CM) apoptosis detected by TUNEL. Compared with mice fed on a normal diet (*ND*) with (**b**) or without (**a**) nicotine (*Nic*) or on high-fat diet (*HFD*) alone (**c**), after which little or no apoptosis was detected, combined treatment with nicotine and HFD (*HFD+Nic*) resulted in a marked increase in the incidence of apoptosis (**d**). Treatment with mecamylamine (*M*) significantly ($P < 0.05$) prevented nicotine-plus-HFD-induced CM apoptosis (**e**). Electron microscopy confirmed the apoptotic nature and the identity of dying cells as CMs (**f**, **g**). *Bar* 25 μm (**a**μ**e**), 2.5 μm (**f**, **g**). **h** Quantitation of CM apoptosis. Apoptotic rate is expressed as the percentage of TUNEL-positive nuclei per total nuclei (apoptotic plus non-apoptotic nuclei) counted in a unit reference area. Values are means ± SEM of 5 mice and were taken from 10 grid fields/reference areas in each of 5 ventricular sections for a total of 50 reference areas per mouse. Means with unlike superscripts are significantly ($P < 0.05$) different. Note the marked increase in the incidence of CM apoptosis in the combined treatment group; this is not seen following mecamylamine treatment

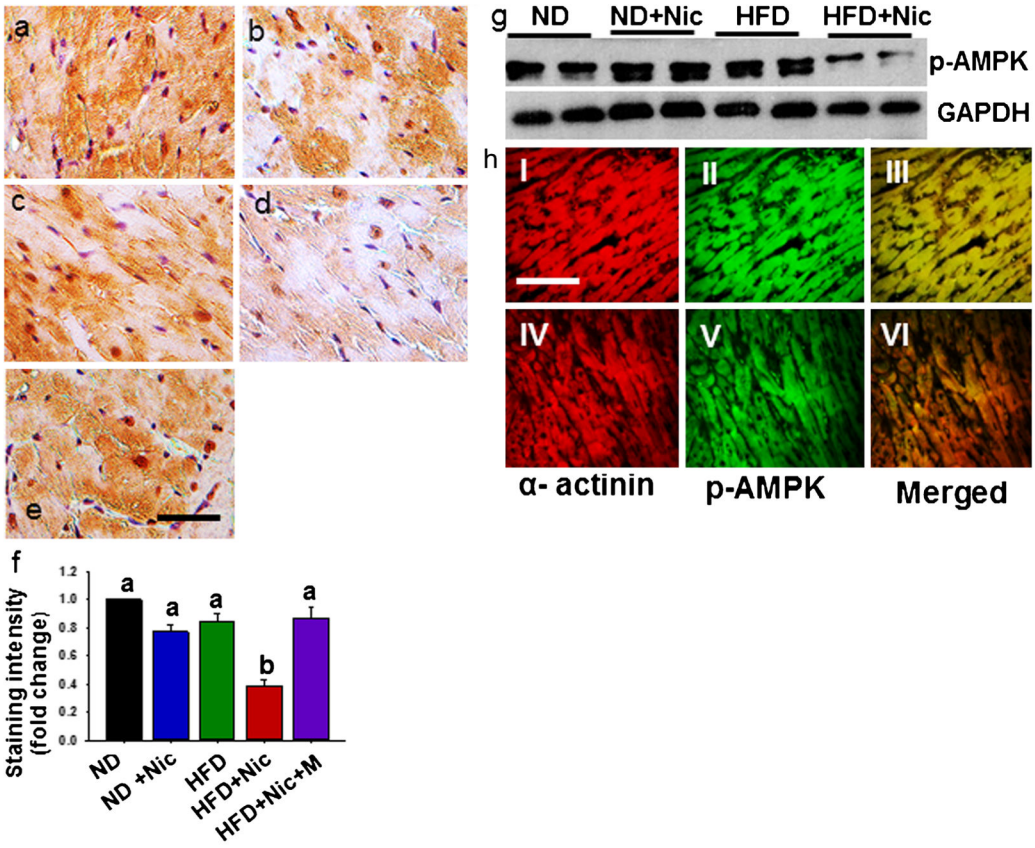

Fig. 2.

Visualization of AMP-activated protein kinase (*AMPK*) inactivation (dephosphorylation) by immunohistochemistry. Compared with mice fed on ND with (**b**) or without (**a**) nicotine or on HFD (**c**), combined treatment with nicotine and HFD results in a marked decrease in phospho-AMPK immunoreactivity (**d**). Treatment with mecamylamine significantly attenuates nicotine plus HFD-induced decrease in phospho-AMPK levels (**e**). **f** Quantitation of staining intensities. Values are means ± SEM of 5 mice and were taken from 10 test areas in each of 5 ventricular sections for a total of 50 test areas per mouse. Means with unlike superscripts are significantly ($P < 0.05$) different (*ND* normal diet, *Nic* nicotine, *HFD* high-fat diet, *M* mecamylamine). **g** Western blot analysis also reveals a marked decrease in phospho-AMPK levels by nicotine plus HFD compared with mice fed ND with or without nicotine or HFD (*p-AMPK* phospho-AMPK, *GAPDH* D-glyceraldehyde-3-phosphate dehydrogenase). **h** Co-staining for α-actinin, a cardiac myocyte marker shows localization of phospho-AMPK in cardiomyocytes in mice fed either ND (*I–III*) or HFD (*IV–VI*). Note the decreased expression of phospho-AMPK levels after combined treatment with nicotine plus a HFD in cardiac myocytes (*IV–VI*). *Bars* 25 μm

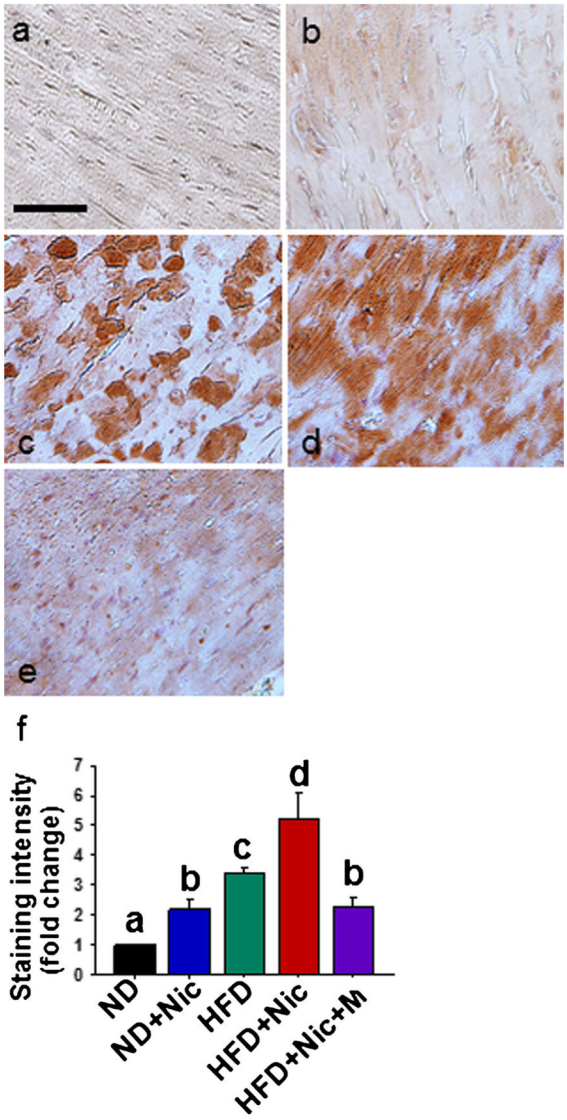

Fig. 3.

Compared with mice fed on ND (**a**), nicotine treatment leads to a modest increase in 4-hydroxynonenal protein adduct (4-HNE) expression (**b**). Nicotine plus HFD causes a greater oxidative stress, as evidenced by elevated 4-HNE levels (**d**), relative to mice on ND with nicotine (**b**) or fed on HFD alone (**c**). Treatment with mecamylamine significantly attenuates the nicotine-plus-HFD-induced increase in cardiac oxidative stress (**e**). *Bar* 25 μm. **f** Quantitation of staining intensities. Values are means ± SEM of 5 mice and were taken from 10 test areas in each of 5 ventricular sections for a total of 50 test areas per mouse. Means with unlike superscripts are significantly ($P < 0.05$) different

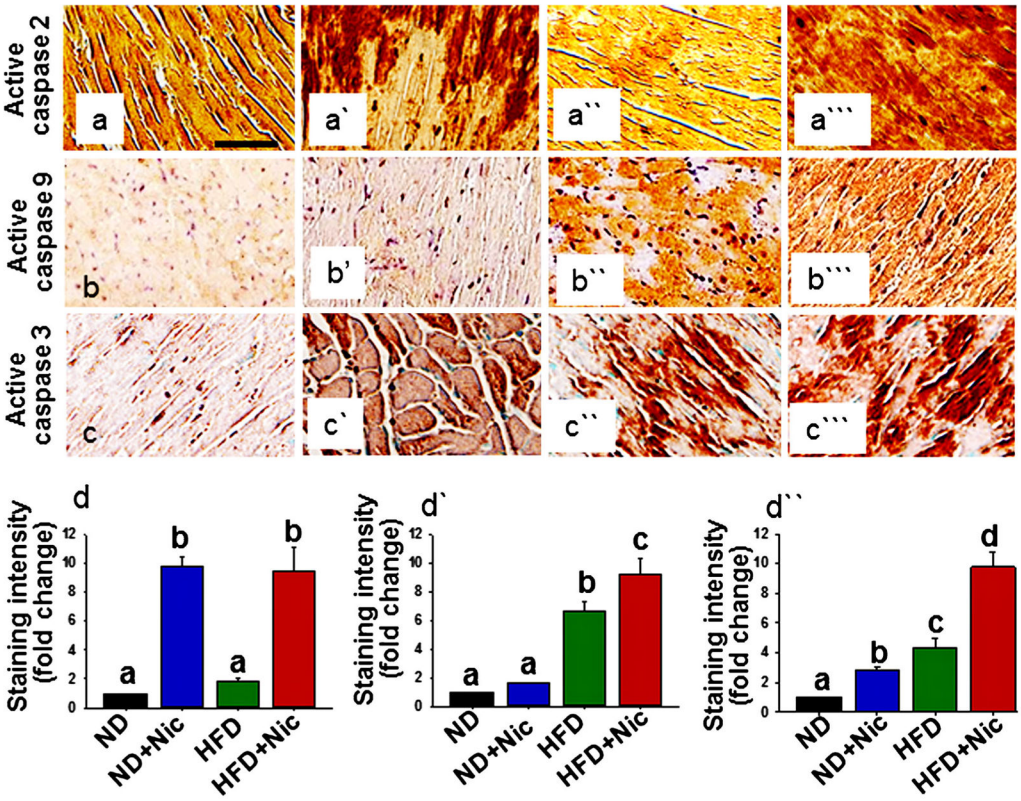

Fig. 4.

Activation of caspase 2 (**a**–**a**‴), caspase 9 (**b**–**b**‴) and caspase 3 (**c**–**c**‴) in ventricles as detected by immunohistochemistry. Nicotine significantly increases ventricular active caspase 2 expression in mice fed either on ND (**a**′) or on HFD (**a**‴). However, caspase 2 activation only in the combined treatment group is associated with activation of downstream caspase 9 (**b**‴) and caspase 3 (**c**‴). *Bar* 25 μm. Quantitation of staining intensities for caspase 2 (**d**), caspase 9 (**d**′) and caspase 3 (**d**″). Values are means ± SEM of 5 mice and were taken from 10 test areas in each of 5 ventricular sections for a total of 50 test areas per mouse. Means with unlike superscripts are significantly ($P < 0.05$) different

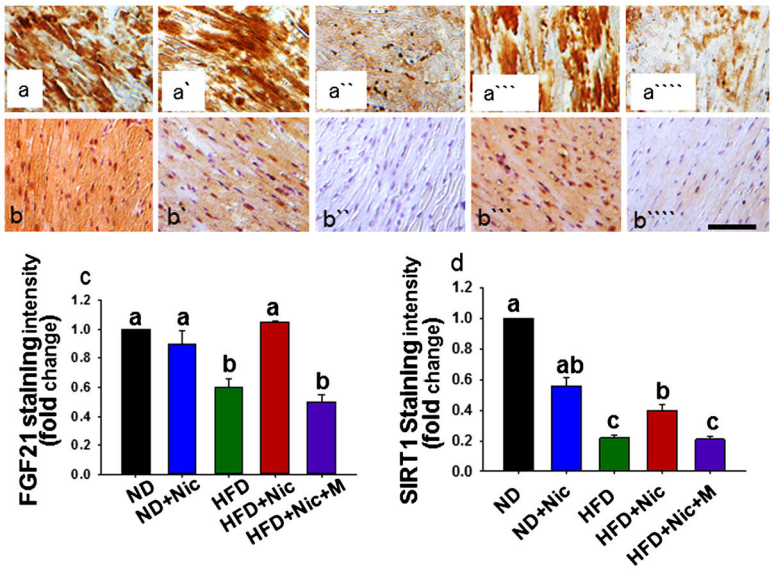

Fig. 5.

Immunohistochemical analysis of ventricular expression of fibroblast growth factor 21 (FGF21; **a**–**a**‴′) and silent information regulator 1 (SIRT1; **b**–**b**‴′). Compared with mice fed on ND with (**a**′, **b**′) or without (**a**, **b**) nicotine, mice on HFD exhibited a marked decrease in the ventricular expression of FGF21 (**a**″) and SIRT1 (**b**″). Combined treatment with nicotine and HFD fully attenuated such a HFD-induced decrease in the ventricular expression of FGF21 (**a**‴) or SIRT1 (**b**‴).

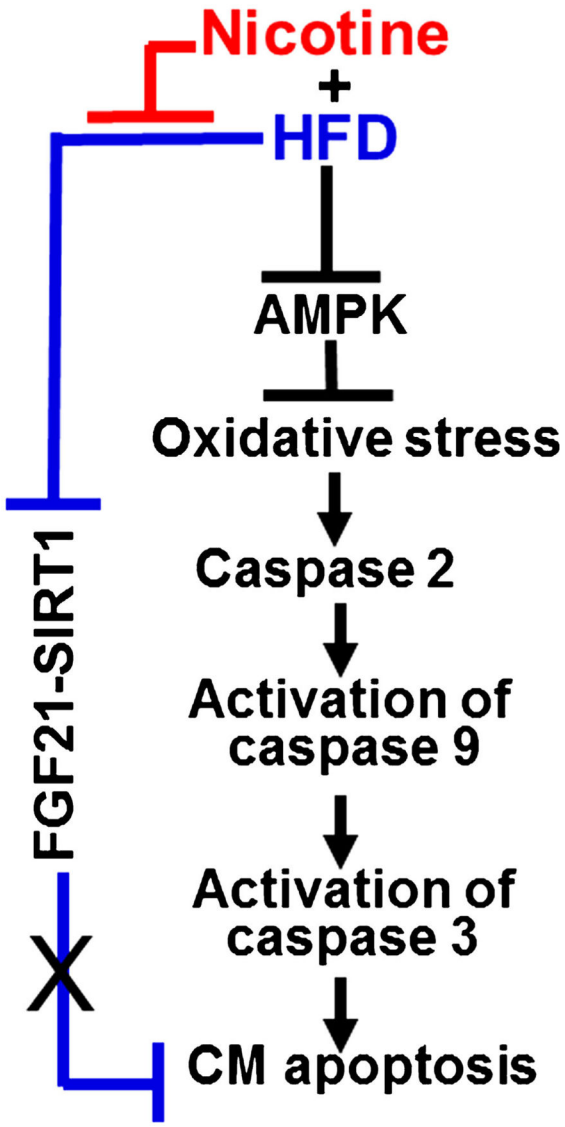

Fig. 6.

Proposed mechanisms by which nicotine when combined with HFD triggers CM apoptosis. Nicotine plus HFD triggers CM apoptosis through inactivation of AMPK, leading to the generation of oxidative stress and the activation of the caspase-2-mediated intrinsic apoptotic pathway. Nicotine is able to restore an HFD-induced decrease in ventricular FGF21 and SIRT1. However, the restoration of ventricular SIRT1 and FGF21 levels in HFD-fed mice by nicotine fails to prevent nicotine-plus-HFD-induced CM apoptosis